

Geotechnical aspects and seismic damage of the 156-m-high Zipingpu concrete-faced rockfill dam following the Ms 8.0 Wenchuan earthquake

Jian-Min Zhang ^{a,*}, Zeyan Yang ^b, Xizhang Gao ^c, Jianhong Zhang ^a

^a State Key Laboratory of Hydroscience and Engineering/School of Civil Engineering, Tsinghua University, Beijing 100084, China

^b Hydropower and Water Resources Planning & Design General Institute, Beijing 100120, China

^c Sichuan Provincial Water Conservancy and Hydropower Survey and Design Institute, Chengdu 610072, China



ARTICLE INFO

Article history:

Received 5 August 2014

Received in revised form

16 February 2015

Accepted 20 March 2015

Available online 9 April 2015

Keywords:

Concrete-faced rockfill dam

Face slab

Earthquake

Damage

Joint

Deformation

ABSTRACT

Damage to the Zipingpu concrete-faced rockfill dam (CFRD) with the maximum height of 156 m was induced by the great May 12, 2008 Wenchuan earthquake with a magnitude of Ms 8.0. The dam is the first CFRD over 150 m high experiencing the strong shallow earthquake of IX degree in the world. The seismic damage to the dam raised a number of questions concerning the safety of the dam as well as the adequacy of design criteria. Extensive investigation has been carried out accordingly and is summarized in this paper. The purpose of this paper is to document geotechnical aspects of the design and seismic damage during earthquake, and in particular to highlight key experiences and lessons learned. Analysis of the instrumental records during the earthquake and results of the subsequent surveys following the quake yield three key conclusions as follows. (1) The earthquake motion mainly caused significant seismic non-uniform deformation of the embankment and damage to the face slabs, structures on the crest and downstream stone masonry. The predominantly longitudinal seismic motion intensified the interaction between the embankment and the abutments. The seismic deformation of the embankment and the strong interaction between the abutments and embankment were believed to have been responsible for damage to face slabs. Seepage through the dam increased, but was not significant, due to water-seal damage in the concrete face and peripheral joints. In general, the damage to the dam, although serious in some parts, was minor as a whole and was reparable. (2) Several design considerations contributed to the safety of the Zipingpu dam. Shallow-angle slopes on the downstream dam face were used to enhance the stability of the dam. Most significantly, the adequate zoning and well-compacted rockfill enabled effective deformation control of the embankment, thus greatly reducing the seismic deformation during ground shaking and ensuring the safety of the seepage control system. The performance of the Zipingpu dam during the earthquake evidenced the success of the design. (3) Overall, the Zipingpu CFRD was structurally stable and safe even though it was subjected to seismic shaking at a greater magnitude than the design seismicity. High CFRDs are feasible in seismic regions of western China if adequate design considerations are implemented to alleviate as much damage as possible during major earthquakes.

© 2015 Elsevier Ltd. All rights reserved.

1. Introduction

China is the country with the largest number of high-embankment dams built in the world. The embankment-type dam has several advantages, including high adaptability to different topographic and geologic conditions, wide availability of materials, and simple and fast construction [1]. It has become

the world's most common type of high dam in recent decades. The concrete-faced rockfill dam (CFRD) is a type of high-embankment dam favored by dam engineers. By the end of 2011, about 600 CFRDs were either completed, under construction or in planning, in nearly 100 countries. About 50% of these are located in China, where there are 48 CFRDs over 100 m high that are complete, 20 under construction and 27 in planning [2].

China is rich in hydropower resources, and about 70% of the total hydropower resources are concentrated in the west of China. However, these regions are well known for their high seismicity, both in terms of earthquake magnitude and frequency. Most of the high-embankment dams in China are built in high seismicity

* Correspondence to: Institute of Geotechnical Engineering, School of Civil Engineering/State Key Laboratory of Hydroscience and Engineering, Tsinghua University, Beijing 100084, China. Tel.: +86 10 62772062; fax: +86 10 627985593.
E-mail address: zhangjm@mail.tsinghua.edu.cn (J.-M. Zhang).

regions, where seismic safety becomes a control factor in design. Before the Wenchuan earthquake, only some embankment dams below the height of 100 m had been subjected to severe earthquake damage. The Zipingpu CFRD is the first dam of this type over 150 m high subjected to a seismic intensity of 9, during the Ms 8.0 Wenchuan earthquake of May 12, 2008. The damage to the dam resulting from the strong and long duration of shaking immediately raised great concerns regarding the safety of the dam and downstream communities [3–5].

Extensive investigations of geological hazards in the reservoir and damage to the Zipingpu dam were conducted [4,6–18]. A description of the investigations and discussions on the Zipingpu dam is presented herein with emphasis on the geotechnical aspects of the design and seismic damage as well as some key experiences and lessons learned. This paper is an extension of the keynote paper published in GeoShanghai International 2010 [19].

2. General description of the Zipingpu hydraulic project

2.1. Project location

The Zipingpu hydraulic project, situated 60 km northwest of Chengdu City, Sichuan Province, is the lowest of the upstream cascade developments in the Minjiang River. It was categorized by the design codes of China to be a first-class large-scale water control project with the main functions of irrigation and water supply, and other benefits from power generation, environmental protection and tourism. The normal reservoir water level is at an elevation of 877 m with a corresponding storage capacity of 1,112 billion m³. The total installed capacity is 760 MW. The project mainly consists of a CFRD, a spillway, two flood discharge and flushing tunnels, a scour sluiceway and a power house with four generator units.

2.2. Geology

The topography of the Zipingpu region comprises low and moderate mountainous terrain formed by tectonic denudation. The CFRD lies on the end of a U-shape river bend, which has been incised by the Minjiang River, as shown in Fig. 1. The dam is in the Shajinba section, downstream of the Minjiang River. The river valley cross-section is an unsymmetrical V shape. The region is underlain by Upper Triassic lacustrine coal grits and shales with a typical flysch sedimentary formation. The rocks are characterized by vertically alternating coarse and fine particles and laterally significant variations in particle size and lithology. About 49% of rocks are medium and fine sandstone, 37% are siltstone and 14% are bone coal or argillaceous shale.

Tectonic movement has produced the Shajinba syncline, fault zones including faults F2, F2-1, F3 and F4, and interlayer shear weakness zones including L8–L14 (Fig. 1). Interlayer crushing weakness zones are well-developed in the syncline. The fault F3, lying 360 m downstream from the dam axis, comprised of mylonite, fault gouge and tectonic lenses of sandstone. The materials are poorly cemented and easily disintegrate on exposure to water. The interlayer shear weakness zones L8–L14 result from strong tectonic deformation where soft shales have been crushed, sheared and dislocated between hard sandstones. The interlayer shear weakness zones are large scale in terms of both length and width.

2.3. Seismicity

China is located between two of the world's large active belts. One belt, seismically very active, passes through the center of the country from north to south and is part of the China-Pacific Seismic belt and the Mediterranean Seismic belt. The other passes

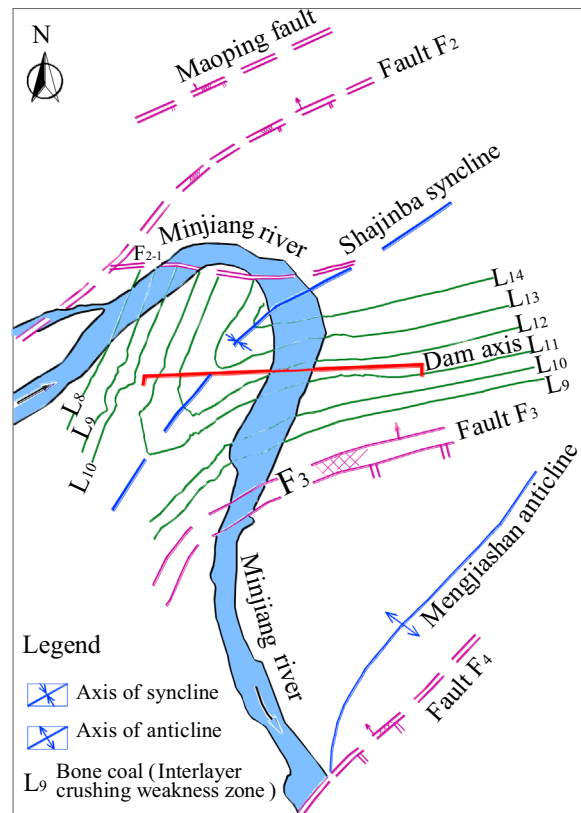


Fig. 1. Geology of the Zipingpu hydraulic project.

through northern China from east to west. The Wenchuan Earthquake of May 12, 2008 resulted from an oblique dextral-thrust motion in the Longmenshan tectonic fault zone within the first seismic belt. The Longmenshan tectonic fault zone is located at the eastern margin of the Tibetan Plateau and adjacent to the Sichuan Basin. This plateau margin may be amongst the steepest, with a relief of 5 km over a distance of less than 50 km, as shown in Fig. 2. It is a major thrust zone that has been repeatedly reactivated in the India-Asia collision. However, historically the maximum earthquake magnitude in this area never exceeded Ms 6.5. It may be the long-term accumulation of energy in the Longmenshan Fault zone that rendered the Wenchuan earthquake the largest event in the past three decades in China. Some studies (e.g. [20–22]) correlated this event with triggering stresses near the Beichuan thrust fault caused by Zipingpu water reservoir, while others (e.g. [23]) suggested that the reservoir probably did not play a role in the occurrence of this earthquake.

3. History of the dam and conditions prior to the earthquake

3.1. Geology and foundation conditions

The general layout of the dam is shown in Fig. 3. A spillway is located on the right abutment. A power house is located on the right base downstream of the dam. The dam rests mostly on recent alluvium consisting of erratic boulders and gravel. However, the alluvium in a zone of about 100 m width downstream from the plinth was excavated as shown in Fig. 4, so that the plinth and half of the upstream dam rests on bedrock. A grout curtain beneath the plinth provides seepage control. The remaining alluvium attains a maximum thickness of 14 m beneath the dam, which was considered to be an acceptable foundation for the dam. Underlying the alluvium are interbedded stiff medium-fine sandstones, siltstone and in some

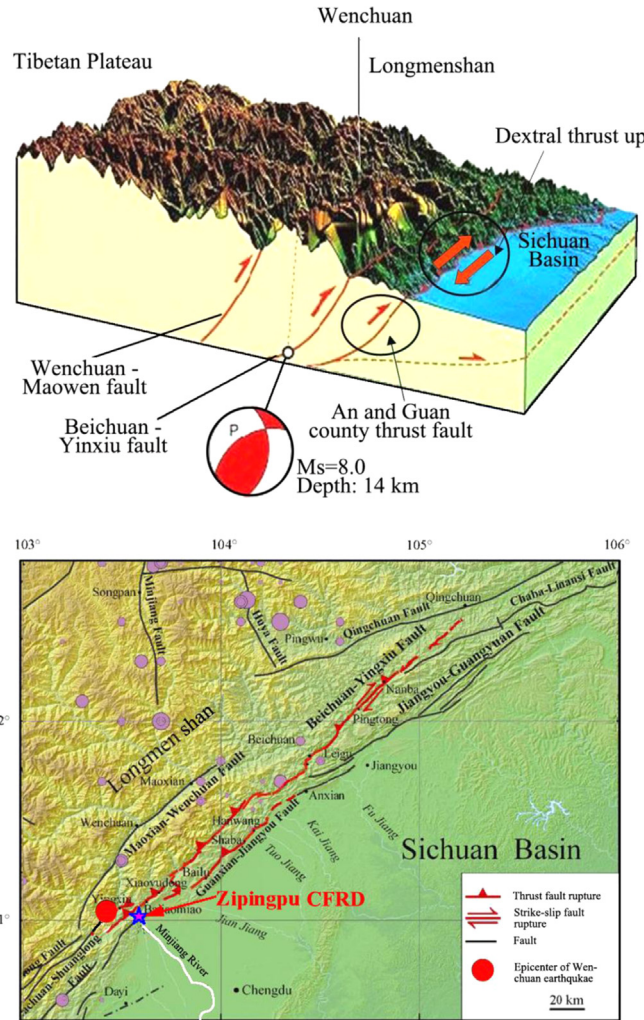


Fig. 2. Thrust motion of Longmenshan tectonic fault zone resulting in Wenchuan earthquake. Minjiang River is shown in white. The figure is simplified from the work of Zou et al. [18].

places bone coal. Fissures are well developed with mainly moderate to gentle dip angles. Five interlayer shear weakness zones L10–L14 are also present in the rocks.

3.2. Design and construction

The Zipingpu dam was designed as a zoned rockfill embankment with a crest 634.8 m long, 12 m wide and 884.0 m in elevation. Its maximum height is 156 m. Fig. 4 schematically illustrates the design of the dam. Construction of the dam began in 2001. It was completed in June 2006. The dam filling mainly comprised medium-hard and hard limestones and partially sandy gravels. A high dry density was achieved by compaction of rockfills, controlled by adopting generally identical compaction techniques in the main, secondary and downstream rockfill zones. Each lift was 900 mm thick and had water added to about 15% by weight; it was then compacted to 800 mm following 8 passes by a 25 t automatic vibratory roller. Following this procedure, the completed embankment was quite uniform, with high strength and low compression as shown in Table 1. The porosity of the limestone rockfill was measured on site to be 18–19% with a corresponding dry density of 2200 kg/m³ to 2270 kg/m³. Equivalent values were 14% for the sand gravels with a corresponding dry density of 2360 kg/m³. The parameters in Table 1 were considered to meet the design requirements.

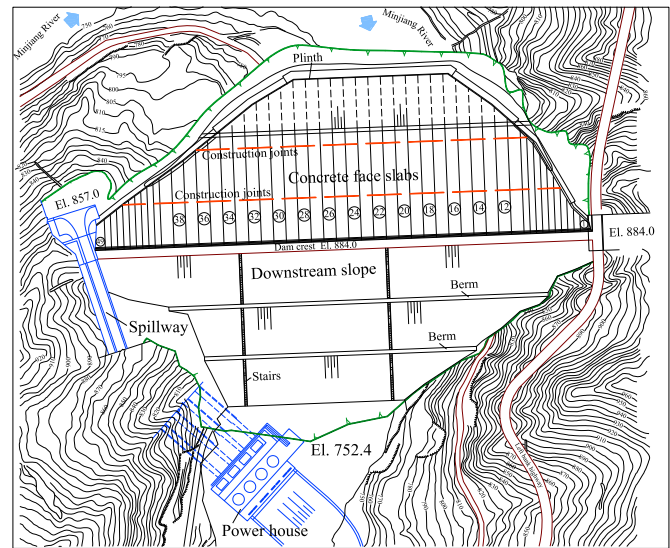


Fig. 3. General layout of the Zipingpu CFRD. (For interpretation of the references to color in this figure, the reader is referred to the web version of this article.)

The concrete face was divided by 48 vertical joints to adapt to the geometry and deformation of the dam embankment. For the 29 compression vertical joints in the central part, smeared bitumen emulsion was used as a water stop for the joint and was underlain by a stripe of copper seal. For the 19 vertical tension joints near the two abutments and peripheral joints, asphalt-smeared spruce planks of 12.5 mm width were placed in the joints and again underlain by a stripe of copper seal. The concrete forming the slab had an unconfined compression strength of 16.7 MPa and a tensile strength of 1.78 MPa. The concrete face was constructed from three stages connected by two horizontal construction joints at El. 796.0 m and 845.0 m, indicated as dashed red lines in Fig. 3.

The seismic design of the dam was based on [27]. As the historical maximum earthquake magnitude in this area was below Ms 6.5, the designed seismic intensity of the Zipingpu dam was determined to be 8. Aseismic considerations are as follows. (1) The downstream slope consists of three parts connected by berms. From top to bottom, the upper slope is shallow and has an angle of 33.7°, while the medium and lower slopes have slope angles of 35.5°. In general, the slope angle is reduced. (2) The secondary rockfill zone was placed downstream from the dam axis, with an inclined instead of upright interface with the main rockfill zone. (3) The rockfills were compacted to avoid sliding failure in seismic conditions. (4) Masonry stones were placed on the surface of the downstream slope and berms to provide surface protection.

In-situ monitoring showed that the maximum settlement of the dam after the construction occurred at El. 790.0 m on the axis, indicating quite a uniform embankment. The maximum settlement reached 881 mm on June 26, 2005, equivalent to about 0.56% of the dam height. The horizontal displacement was downstream-oriented after the reservoir impoundment. When the water level in the reservoir reached El. 874.0 m in October 2006, which is close to the normal water level, recorded displacements were found to change suddenly under the water pressure. The deformation then gradually stabilized.

4. Seismic intensity at the dam site on May 12, 2008

On May 12, 2008, a major earthquake struck Wenchuan County, Sichuan Province and has been assigned a Richter magnitude of 8.0 by the China Seismological Bureau. The focal depth of the Wenchuan earthquake was 14 km and the maximum epicentral

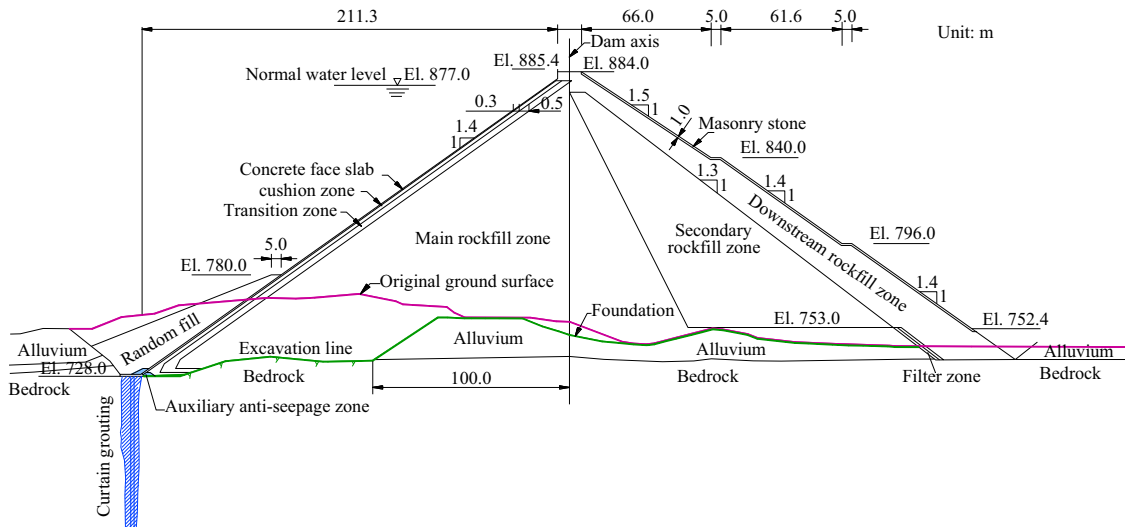


Fig. 4. Maximum cross section of the Zipingpu CFRD.

Table 1
Parameters of materials used in the Zipingpu dam [24–26].

Materials	Internal friction angle obtained in laboratory (°)			Compression modulus (MPa)		Permeability (m/s)	
	Linear		Nonlinear	Lab test	Derived from in-situ test	Lab test	In-situ test
	φ	φ_0	$\Delta\varphi$				
Cushion	38–42	59.5	12.1	155–359	—	$A \times 10^{-4}$ – $A \times 10^{-5}$	1.89 – 6.7×10^{-5}
Filter material	38–41	58.9	12.57	210–241	—	$A \times 10^{-3}$	0.24 – 0.71×10^{-2}
Rockfill	39–40	57.61	11.89	168–245	125–210	$A \times 10^{-2}$ – $A \times 10^{-3}$	1.1 – 3.8×10^{-2}
Sand and gravel	—	—	—	—	—	—	2.2 – 2.5×10^{-4}

$A=1$ –9.

intensity reached 11°. The rupture was about 300 km long and 20 km deep. The total shaking time lasted 80 s. Meanwhile, significant upward movement along one side of the Beichuan-Yingxiu fault aggravated the damage [9,10]. The Zipingpu dam lies about 17 km southeast of the epicenter and 8 km from the surface rupture zone. The main shock of the earthquake at the dam site lasted for 40 s. The seismic intensity at the dam site reached 9, as shown in Fig. 5, greater than the design intensity of 8.

Acceleration responses were recorded by a seismograph installed on the crest of the downstream slope, as shown in Fig. 6a. The China Seismological Bureau later claimed that the instrument was in the process of repairing at the time of the earthquake. However, the recorded responses did demonstrate two predominant seismic motions in the longitudinal and vertical directions. It was the longitudinal seismic motion that intensified the interaction between the embankment and the abutments. Following the earthquake, the China Seismological Bureau recommended an input motion at the base of the dam as shown in Fig. 6b with a new standard of design earthquake, comprising a horizontal peak ground acceleration of 0.392 g with an exceeding probability of 2% in 100 years, and a vertical acceleration of two-thirds of the horizontal acceleration [5]. The response spectrum for design before the earthquake [28] was also included in Fig. 6b for comparison.

5. Major earthquake damage

At the time of the earthquake, the water level in the reservoir was at El. 828.74 m, close to the dead water level of El. 817.0 m. The reservoir was only half-filled due to the pre-flood decrease of

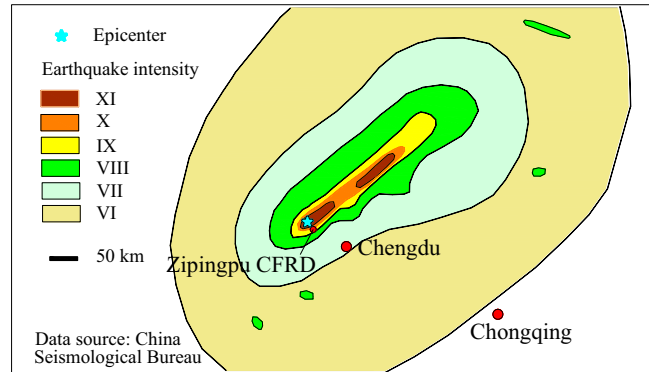


Fig. 5. Seismic intensity distribution of Wenchuan earthquake.

storage. The lowered water level greatly helped in preventing secondary disasters for nearby communities. Two generator units were in operation, each having a capacity of 130 MW.

5.1. Major geological hazards in the reservoir

A small number of rolling stones and landslides were induced by the earthquake shaking above the excavation line on both banks in the reservoir. The colluvial deposits on the left reservoir side slopes near the dam moved toward the reservoir. Three small scale landslides named D1, D2 and D3 were observed at El. 845.0–890.0 m, as shown in Fig. 7a [12]. The landslides were composed of clays and crushed stones. The volumes of landslides D1, D2 and D3 were estimated to be 600, 400 and 150 m³, respectively. Meanwhile, surface cracks were found on highways in the reservoir region at El.

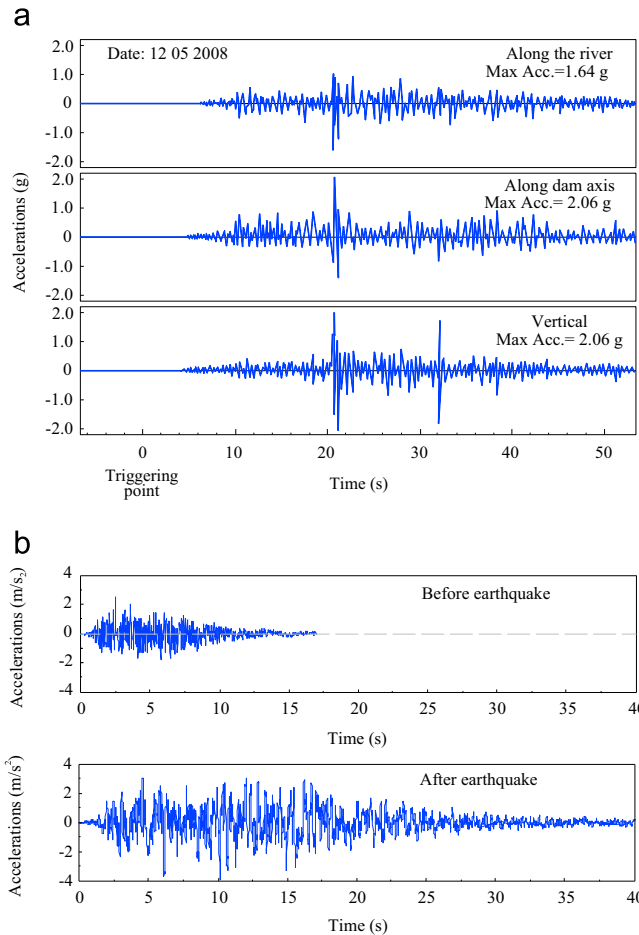


Fig. 6. (a) Recorded acceleration responses on dam crest, (b) acceleration time history for design before earthquake and recommended after earthquake.

890.0 m, as shown in Fig. 7b. No other failures were found in the vicinity of the dam. Both abutments of the dam were stable. Post-earthquake surveys revealed a 2–3 m surge in front of the dam during the earthquake, causing heavy casualties on both banks. However, the safety of the dam was not affected. No liquefaction was found in the overburden layer of the dam foundation.

5.2. Dam crest

During the shaking of the dam, the sluice gate building suffered a range of damages. Parapet walls at the upstream edge of the crest were compressed along vertical joints in the centre and near the right abutment, as shown in Fig. 8a. Surface concrete was crushed, causing spalling and bulging. The parapet walls near the left abutment were pulled open along vertical joints. Some concrete in the wall was crushed. There was 100 mm of dislocation between the top of the spill way and the top of the parapet walls. A 200 mm differential settlement was observed at the junction between the crest and the spillway (Fig. 8b). Cracks with maximum widths of 60 mm developed at the junction of the left abutment, as shown in Fig. 8c. Meanwhile, most of the parapet walls became detached from the adjacent roadway, with a maximum opening of 30 mm. The elevation of the top of the parapet wall was 885.4 m before the earthquake and had decreased to 884.38 m after the event. The maximum settlement was 1.02 m. The road surface became detached from its curb stones along the 500 m-long sidewalk on the downstream side. As shown in Fig. 9a, most of the 550 m-long downstream concrete safety guards collapsed; only those near the right abutment remained. The drop in elevation of the concrete was

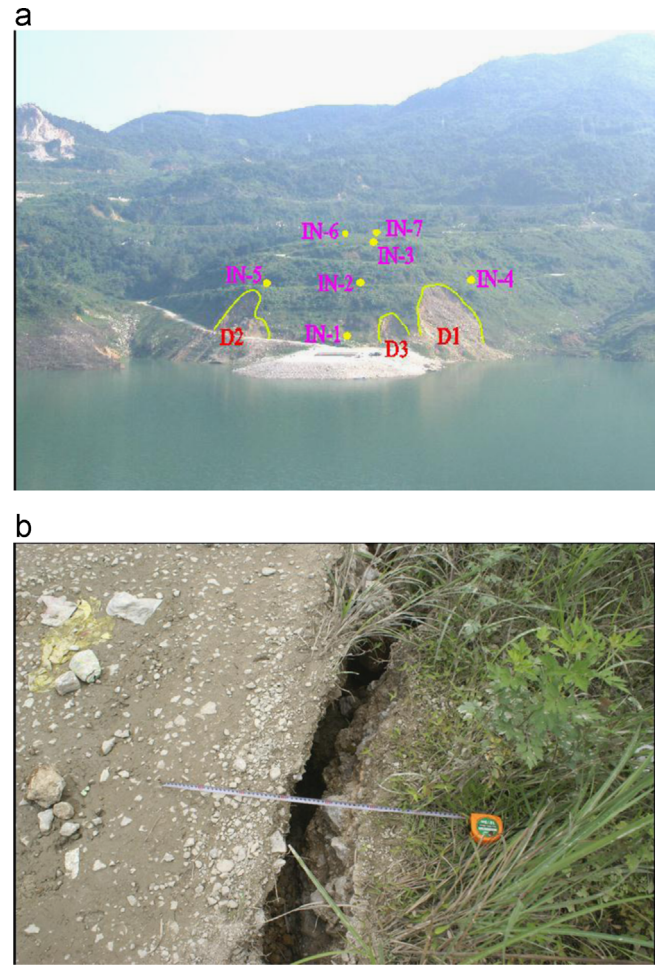


Fig. 7. Geological hazards in reservoir: (a) landslides and (b) surface crack on reservoir highway [23].

measured from its original location and is illustrated in Fig. 9b. Almost all safety guards were broken at the bottom and were moved perpendicular to the dam axis.

5.3. Upstream surface (anti-seepage system)

Fig. 10 shows the upstream surface of the Zipingpu CFRD after the Wenchuan earthquake. The surface features indicating the nature of damage to concrete face slabs include arching, bulging, detaching and cracking with several penetrating cracks on the upstream face slab nos. 3–8, 10–12, 15, 17–25, 27, 28 and 36. The horizontal construction joints defining the second and third stages experienced extensive dislocations (Fig. 11), which were resulted from excessive residual shear strain or permanent deformation of the rockfill ([29,30]) and affected by water elevation in the reservoir [18]. The total length of dislocation was up to 340 m and the maximum dislocation was 170 mm. The steel rebar was bent due to relative movement of the slabs. For example, dislocations of 150–170 mm were observed on slab nos. 5–12; 120–150 mm on slab nos. 14–23; and 20–90 mm on slab nos. 30–42. Moreover, cracks developed at the construction joints on slab nos. 30–34 and 39–42 at El. 845.0 m.

In addition to the dislocations along the construction joints as previously described, severe dislocations also developed along the vertical joints. For instance, the dislocation between face slab nos. 5 and 6 reached 350 mm and the concrete on both sides of these slabs suffered from compression damage from El. 880.4 m to El. 845.0 m. The dislocation between face slab nos. 23 and 24 extended

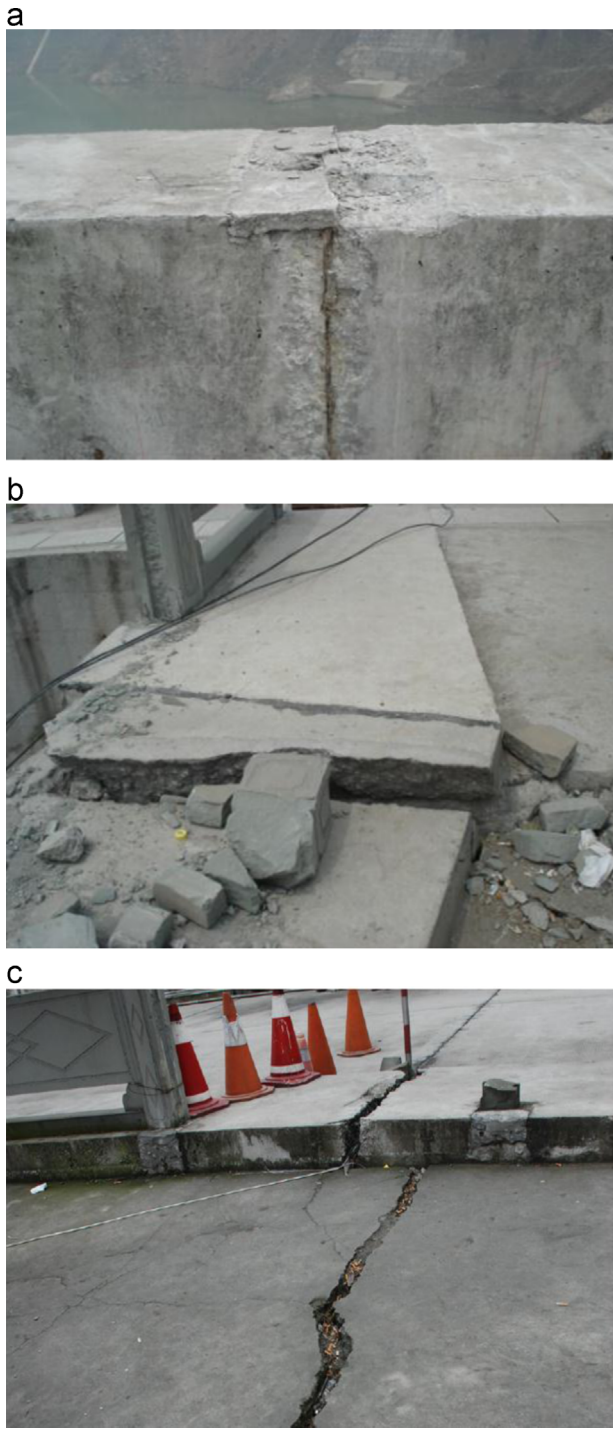


Fig. 8. Damages to the crest: (a) squeezing of vertical joint between parapet walls, (b) differential settlement between crest roadway and spillway, and (c) cracks at left abutment [12].

from the top to the underwater elevation of 791.0 m with a maximum dislocation of 150 mm and damaged length accounting for 60% of the total length of the slabs. As shown in Fig. 12, the concrete of slab no. 23 was compressed with a damage width of 0.5–1.7 m. A borehole inspection of slab no. 23 at El. 843.0 m also indicated that the damaged depth of the concrete was 320 mm and that a cavity of 50 mm in dimension had formed. The mesh reinforcement that had been installed within the edges of the slabs was detached from its protective concrete layer.

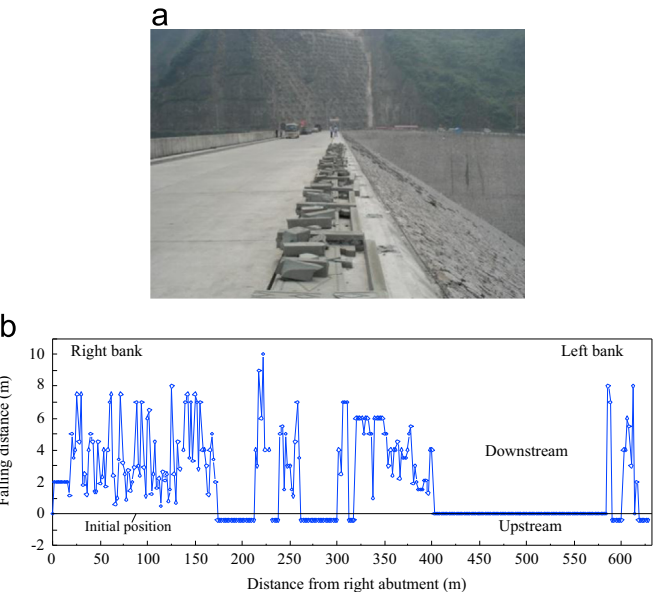


Fig. 9. (a) Collapsed concrete safety guards and (b) falling distance of safety guards.



Fig. 10. Upstream surface of the Zipingpu dam after earthquake [12].

5.4. Downstream slope

The masonry stones on the downstream slope below the crest curb stone slid downstream, leaving a gap between them with a maximum width of 650 mm. A close-up view of this area is shown in Fig. 13. Large areas of masonry stones near the right abutment were uplifted. Those adjacent to the berms at El. 840.0 m and 796.0 m were loosened and displaced. Those within El. 780.0–790.0 m and below the berm of El. 796.0 m were uplifted and loosened. Some scattered stones below the berm of EL. 840.0 m fell off.

6. Major monitoring results

6.1. Exterior deformation

Displacements were recorded at a number of locations on the dam surface, indicating the deformation of the dam during the earthquake relative to data collected before the earthquake (in April 2008). Fig. 14, an elevation view from the downstream direction, illustrates lateral displacements and settlements of the downstream slope surface. The short lines in dull red with arrows

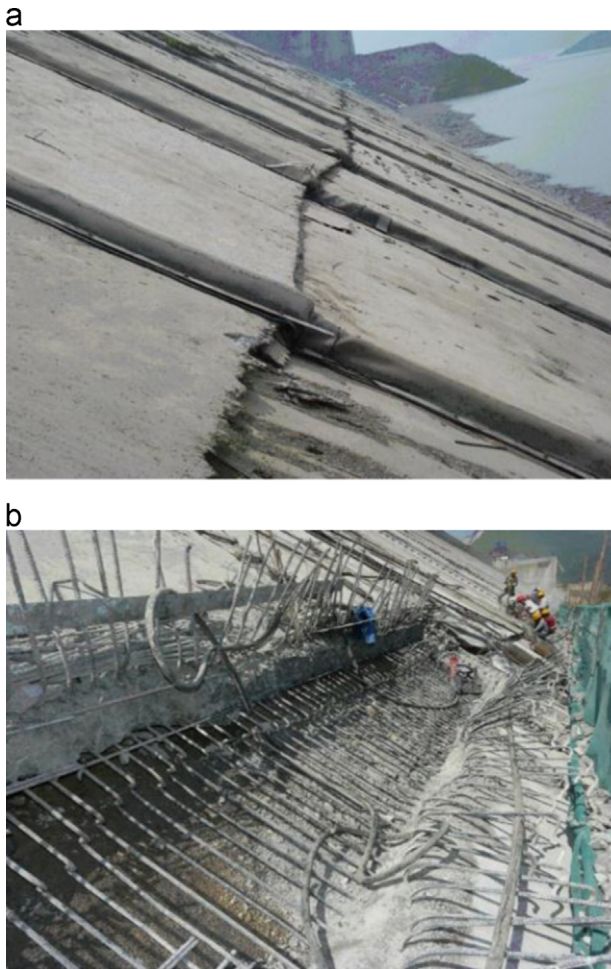


Fig. 11. Damages to construction joints at El. 845 m: (a) dislocation at the joint and (b) excavation of the joint [12].

in Fig. 14a designate two components of lateral movement at each measuring point, i.e. the longitudinal movement X parallel to the dam axis and the downstream movement Y pointing downward. The downstream lateral movements of the crest, the upper berm at El. 840.0 and lower berm at El. 796.0 are illustrated by red, blue and green lines in Fig. 14a, respectively. This figure clearly shows that the entire body of the dam participated in the movement downstream. The maximum downstream lateral displacement of 270.8 mm occurred at measuring point M20, near the upper berm at El. 840.0 m.

The upper parts at the two ends of the dam were two zones with the most significant lateral displacement in the longitudinal direction, as shown in Fig. 14a. The maximum displacement at the left bank was 226.1 mm, while it was 106.8 mm at the right bank. One important feature was that the dam moved laterally toward the centre from both of its two ends in the upper part, resulting in compression at the centre. Nevertheless, the upstream surface was being twisted at the time of the earthquake, as below the upper berm at El. 840.0 m, lateral movement was characterized mainly by a component toward the right bank. This component exhibited the greatest value of 158.4 mm near the left abutment (at Measuring Point M17) and decreased gradually from left to right. As a result, the dam was pushed from both abutments but with greater thrust forces from the left. It evidenced the strong interactions of the abutments and embankment and was believed to be responsible for damage to face slabs and downstream stone masonry.



Fig. 12. Damages to No. 23 slab: (a) squeezing damage to concrete and (b) excavation of the damaged concrete [12].



Fig. 13. Gaps between dam crest and downstream stone masonry [12].

One of the major effects of an earthquake is settlement of the dam embankment [31–33]. Significant settlements were recorded instantaneously by settlement meters that had been installed on the surface. Fig. 14b depicts the movements of the crest, the upper berm and the lower berm. The maximum settlements took place at the crest of the dam, especially in the central part. A maximum settlement of 744.3 mm was recorded at Measuring Point M7 in the central parapet wall on May 17, 2008. This increased to 760 mm in the 45 days following the earthquake. Although the dam kept on settling, the rate of settlement decreased rapidly during the first few days following the earthquake, as shown in Fig. 15. In general, the significant deformation of the dam embankment was crucial for the damage

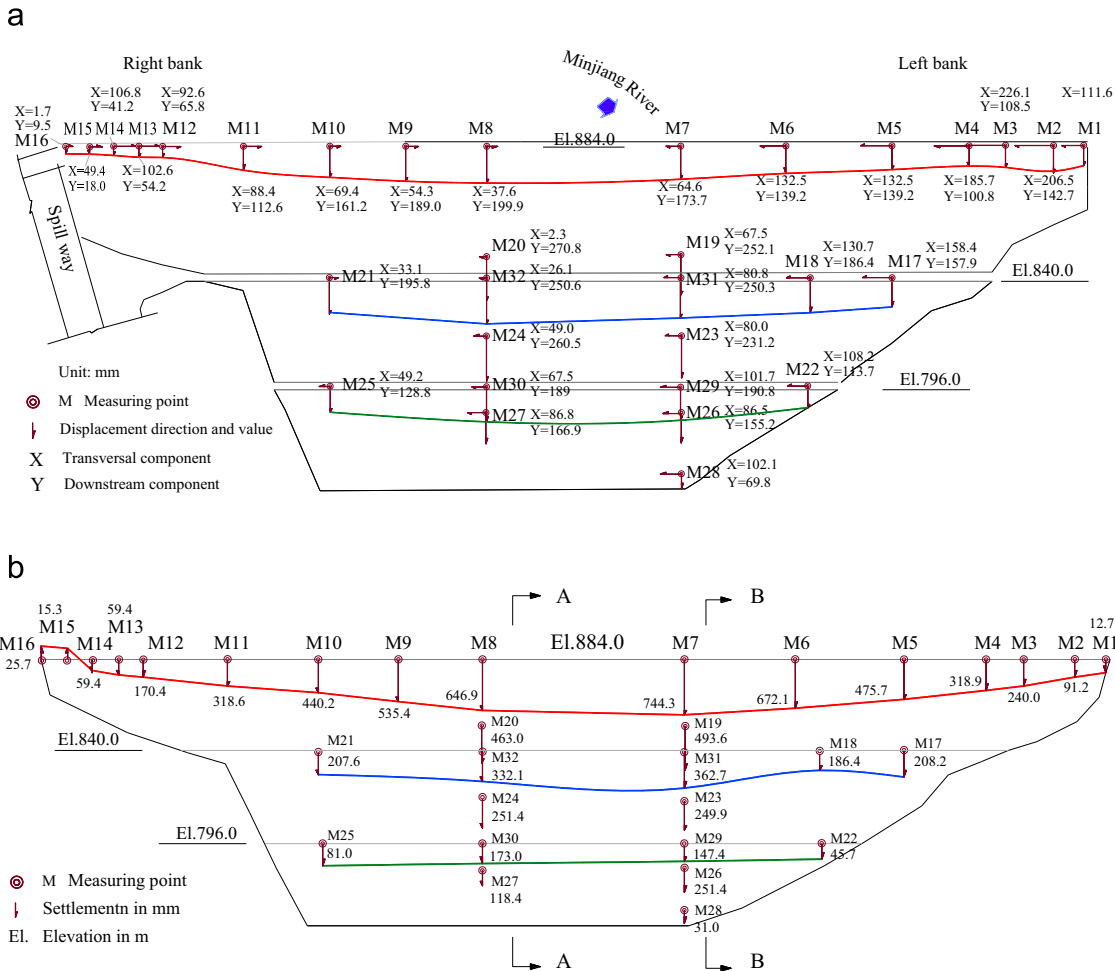


Fig. 14. Movement of the downstream slope surface (relative to data in April 2008): (a) lateral movements and (b) settlements. (For interpretation of the references to color in this figure, the reader is referred to the web version of this article.)

to face slabs. Detailed analyses in this respect were provided in relevant studies [29,30,34].

6.2. Interior deformation

The instruments installed inside the dam provided valuable information for engineers to study the performance of the dam during earthquake shaking. Records obtained in two cross sections A and B (Fig. 14b), 371 and 251 m from the left bank, indicated lateral downstream movement, which is identical to the movement at the surface as described above. The maximum lateral displacement was recorded as 179.7 mm at a measuring point 90 m downstream from the dam axis. A range of 146–165.5 mm lateral displacement was recorded at the other locations. However, at several locations the records were not available as the displacements exceeded the range of the instruments.

Settlements recorded in the two cross sections A and B are depicted in Fig. 16, showing values on May 19, 2008 relative to those on May 12, 2008 just before the earthquake. The units of settlement are millimeters, other dimensions are in meters. The two cross sections exhibited primarily identical characteristics. Settlements at El. 840.0, 820.0, 790.0 and 760.0 m are characterized by red, blue green and brown lines in Fig. 16, respectively. Features of the settlement can be summarized: (1) the settlement was greatest in the upper central part and decreased from top to bottom. It was slightly greater in the downstream than those in the upstream, due to the downstream mass movement of the embankment. (2) As

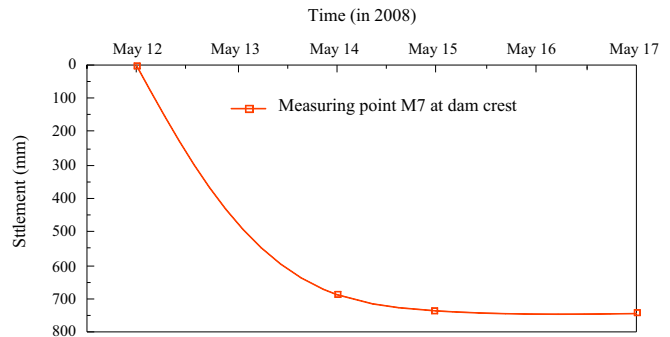


Fig. 15. Recorded settlements at dam crest after earthquake.

discussed previously, more significant abutment–embankment interactions took place at the left bank. The effect resulted in greater settlements in cross section B, which was located at the left side of the dam than those in cross section A. The maximum value, of 810.3 mm, was recorded at El. 850.0 in cross section B (Fig. 16b).

6.3. Joint displacement

Joint gauges were installed during construction of face slabs. Fig. 17 shows the locations of the gauges. There are three sets of joint gauges, comprising one-dimensional and two dimensional gauges at the vertical joints between face slabs, and three-dimensional joint

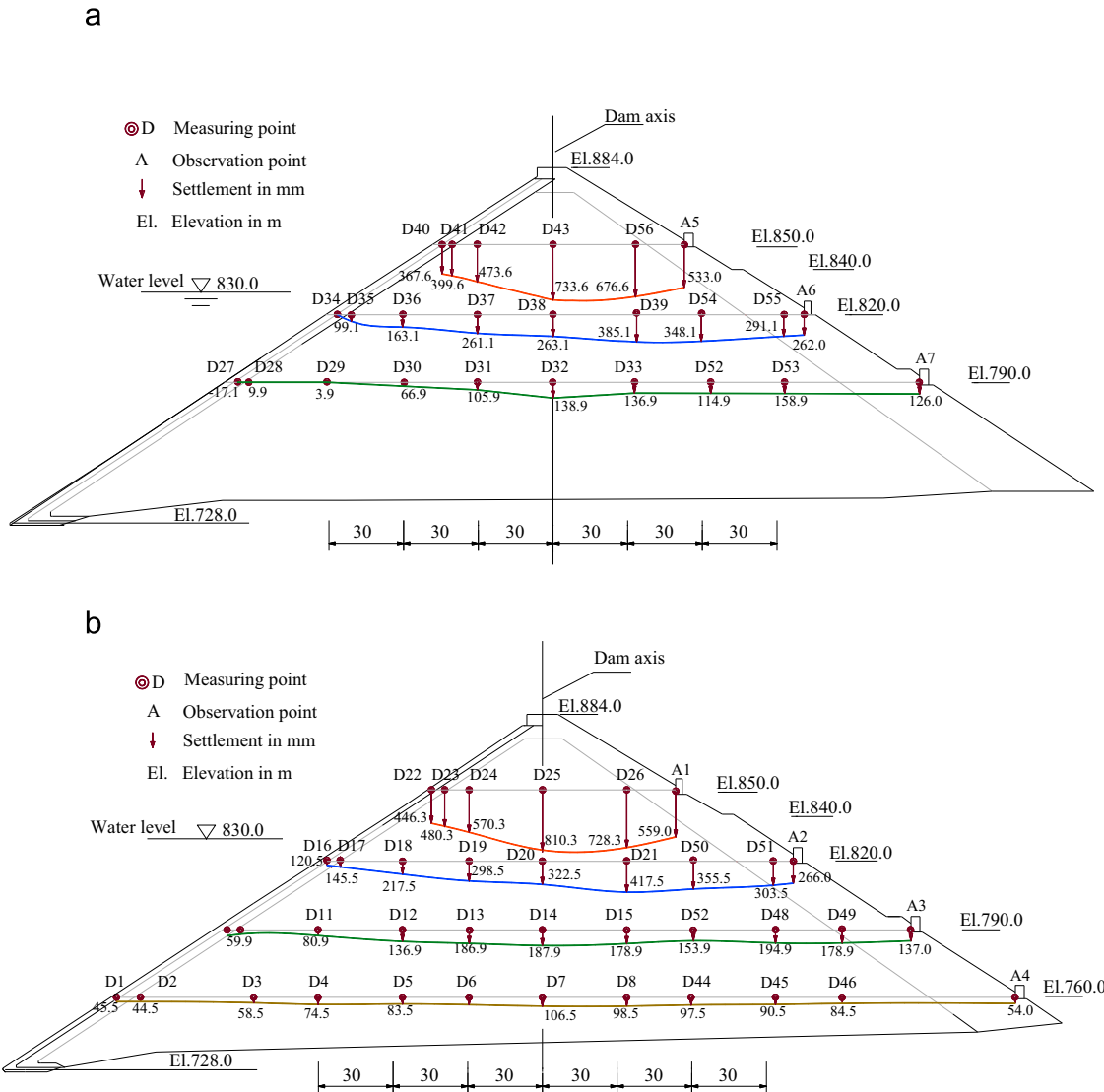


Fig. 16. Settlements on May 19, 2008, relative to May 12, 2008, before earthquake: (a) cross section A and (b) cross section B. (For interpretation of the references to color in this figure, the reader is referred to the web version of this article.)

gauges at the peripheral joints. Some of the gauges were broken during the earthquake and did not record data.

The peripheral joint at Observation Point Z2, El. 833.0 m, on the left abutment, was observed on May 13, 2008 to have an opening of 57.85 mm, a shear displacement of 13.42 mm and a settlement of 92.85 mm at the joint. At the toe of the dam (Observation Point Z9) on the right riverbed at El. 745.0 m, a settlement of 53.65 mm was observed on May 18, 2008 along with an opening of 26.97 mm and a shear displacement of 103.77 mm at the joint. The displacements of the peripheral joints at some locations exceeded the allowable values of the joint gauges.

The joints between concrete slabs were found to deform due to the seismic shaking. Because of the complex stress conditions of the slabs, both tensile and compressive deformations were recorded at the joints by the gauges. Fortunately, the deformations did not exceed the allowable ranges of the watertight materials.

6.4. Separation between concrete slabs and the cushion layer

A set of instrumental records was provided by two-dimensional dislocation gauges that had been installed immediately under the face slabs, as shown in Fig. 17. This data set indicated separations between the face slab and the cushion layer during the

earthquake. Unfortunately, as half of the gauges were broken in the strong shaking, it was difficult to assess the characteristics of this kind of dislocation. Therefore, a post-earthquake borehole inspection was conducted to examine 18 face slabs at 5 elevations: El. 833.0 m, 843.0 m, 847.0 m, 860.0 m, 878.0 m and 879.0 m. It was found that above El. 845.0 m, separations were severely developed in face slab nos. 1–23 and partially developed in the top sections of face slab nos. 24–49. At El. 879.0 m, a significant separation of 230 mm occurred at the top of the face slab no. 6. Separations of 210 mm and 180 mm were observed in face slab nos. 15 and 19, respectively, and of 170 mm in slab nos. 17, 21 and 23, respectively. The separations recorded in the other slabs were less than 120 mm. Below El. 845.0 m, no separation was found except in slab no. 6, which had a separation of 20 mm at El. 833.0 m.

6.5. Seepage

Three sets of 10 vibrating wire osmometers were installed inside the embankment. They were located at the peripheral joints, within the cross section B (Fig. 14b) and in the two abutments. Only three osmometers at the toe of the dam broke during the earthquake. The instrumental records showed that the downstream seepage flow was

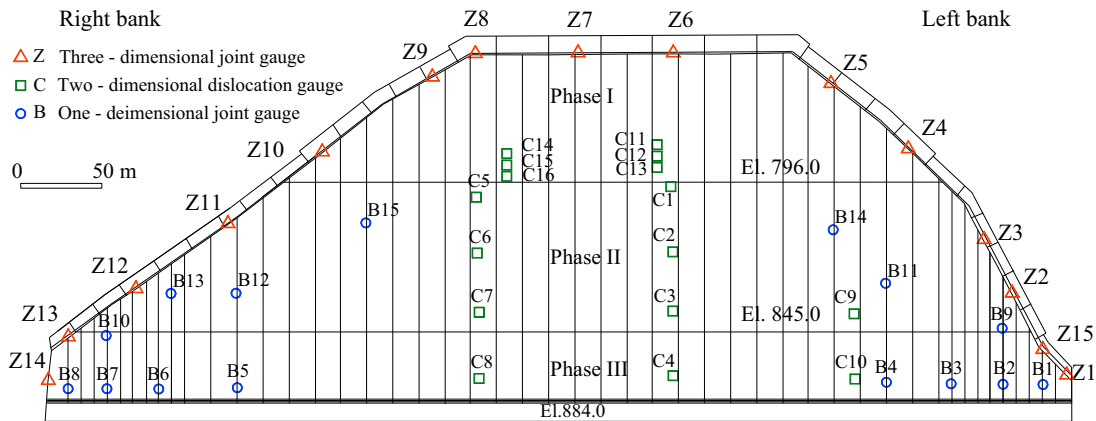


Fig. 17. Placement of joint gauges on the upstream slope of the dam.

17 L/s at the level of El. 820.0 m (on May 10, 2008) before the earthquake. This increased to 25 L/s at the reservoir level of El. 835.0 m (on May 20, 2008) then decreased with the water level following the earthquake until early June, as shown in Fig. 18. The seepage flow was turbid with silt in the first two days following the earthquake but then became clear. No significant increase of bypass seepage was observed in the two abutments following the quake. This indicated that the seepage control system was still effective and that the overall structure of the dam was safe and stable. The water level in the reservoir was then allowed to rise after June 6, 2008.

7. Discussions

7.1. Main features and evaluation of earthquake-induced damage

The Zipingpu dam experienced ground shaking much stronger than the design seismic intensity. The dam crest suffered significant damage and deformation. Major seismic subsidence and lateral downstream displacement of the dam body were induced by the quake. Meanwhile, the seepage control system was severely damaged from the compression, separation and dislocation of the face slabs. Large areas of the masonry stones on the downstream slopes were loosened and overturned, and a few rolling stones were found on the slopes of both banks.

Some features of the seismic damage can be summarized as follows. (1) The damage to the upstream surface was more severe, owing to its shell structure, than damage to the downstream surface. (2) The damage to the upper part of the dam was more serious than damage to the lower part, due to stronger seismic responses in the upper section. (3) Damage to the dam above the water level in the reservoir was greater than damage below the water level. (4) Damage to the left bank face slabs was more significant than damage to the right bank face slabs because of the greater movement at the left bank.

Fortunately, thoughtful dam design and location prevented more severe damage. As previously described, the dam lies centrally between the two closest faults F2-1 and F3 (Fig. 1). The reactivated faults during this earthquake were 17 km away from the site and did not exert a direct impact on the dam. Despite the serious surficial damage to structures such as the dam crest, the face slabs and watertight joints, the dam still functioned well as a water storage system.

7.2. Deformation characteristics

Under the strong seismic action in the main earthquake and subsequent aftershocks, significant deformation occurred within the dam embankment. One major effect of the strong shaking of the

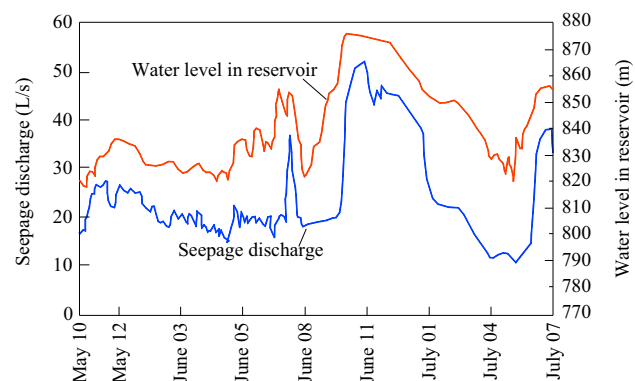


Fig. 18. Seepage discharge and water level in reservoir following the earthquake.

embankment was densification. The surface records showed substantial dam settling, and movement downstream and toward the right bank. Thrust forces were exerted by both banks, which resulted from predominant longitudinal seismic motions. Obviously, a greater thrust force was exerted by the left bank. The strong abutment-embankment interaction and significant seismic deformation of the embankment led to complicated damage patterns of the face slabs [29,30,34].

The settlement recorded by water-tube settlement gauges within cross section B reached 812.5 mm, and 760 mm at the parapet wall on the dam crest. The crest of the parapet wall settled by 1.02 m. Nevertheless, the maximum settlement did not exceed 1% of the maximum dam height, indicating that the rockfills of the dam had a high density or high compression modulus. The design of the zoning was adequate. Adopting identical compaction levels is crucial for zoned rockfills if they are to resist such strong seismic motions.

7.3. Safety against failures

The upstream slope was stable in the earthquake. No surface movement was found owing to the protection of the concrete face slabs and the action of hydraulic pressure. Although two large pieces of the masonry stones on the downstream slope were loosened and overturned during the quake, no significant sliding was produced. The downstream slope remained stable. This may be attributed to high strength of the rockfill and the use of shallow-angle slopes in the upper section. There is no evidence of liquefaction in the foundation alluvium, since lenses of sand had been stripped off prior to placing the embankment fill.

Although the concrete face slabs near the joints suffered severe damage, the downstream seepage did not increase significantly, indicating that current design of the face slabs and watertight

joints is adequate. The seepage increase following the earthquake may be attributed to two reasons: compression damage to the underwater face slabs, and seepage through fissures in the bedrock or cracks in the curtain grouting that developed during the earthquake. The seeping water was turbid with silt in the first two days following the earthquake and became clear afterward, which indicated that the filtration system within the rockfill functioned well. In general, the design concept of the modern CFRD seepage control system is considered to be adequate. The rockfills are resistant to seepage failure.

Compared with the Kegaodianshan CFRD in Chile, which has a height of 84 m and has experienced four strong earthquakes, the Zipingpu CFRD presented similar seismic performance. It is noted that the Zipingpu dam has a greater height and experienced a higher seismic intensity. The instrumental records during the quake and the subsequent surveys following the quake show that high CFRDs with adequate design and a high quality of construction, such as thin layer placement of rockfill and heavy compaction, can effectively withstand the damage caused by major earthquakes.

7.4. Ground motion

The maximum design acceleration at the base of the dam was determined to be 0.26 g. The recorded maximum acceleration at dam crest was around 2.0 g (Fig. 6), from which it was estimated that the acceleration at the base of the dam was probably above 0.50 g, much higher than the design value. Fortunately, the preferred acceleration was not along the river, i.e. the downstream acceleration was smaller than that in the vertical and longitudinal directions. The angle between the main shock and the dam axis was small, so the lateral seismic motion was imposed from the upstream right bank and mainly along the dam axis. In addition, field surveys show that although the dam lies only 17 km from the epicenter, it is located at the footwall of the causative fault, thus greatly alleviating the seismic effects on the dam embankment.

However, there was a big difference in the seismic input between that specified in the existing design code of China and that experienced at Zipingpu. The unique seismic wave propagation characteristics significantly intensified the dynamic interaction between the dam and the abutments, leading to the dislocation and non-uniform deformation of the dam near the abutments. As a consequence, damage to the upstream surface was more serious than damage to the downstream surface, and damage to the slabs on the left bank were more significant than damage to slabs on the right bank. In addition, the whiplash effect was clearly shown by the more serious damage in the upper section of the dam than that in the lower section. Traveling waves may have caused the collapse of the safety guards and the irregular damage to the crest during the quake.

7.5. Weak points susceptible to failure

Field surveys have identified several weak points that may be susceptible to failure during earthquakes: water stop joints, construction joints, and the hard–soft junction between the spillway (hard concrete) and the right end of the embankment (soft rockfills). It is essential to avoid the hard–soft junction design, as the two adjacent portions respond quite differently to seismic motion and thus may suffer significant damage. It is advantageous to have more flexible joints in the face slabs to buffer the dynamic impacts and to adapt to large deformations. The lateral construction joints are considered sub-optimal and may be replaced by vertical construction joints. Further study is needed to tackle these technical problems in the future.

7.6. Reparability

For tall dams such as the Zipingpu dam located in regions of high seismicity, the seismic design is based on the concept of minimizing earthquake damage as much as possible and ensuring that most of the damage is readily repairable. The performance of the Zipingpu Dam demonstrates this concept. By the end of October 2008, most damage had been repaired with the exception of the safety guards at the crest and the downstream slope surface. Water level was then increased to El.860.0 m and the project resumed its normal operation.

8. Conclusions

This paper describes some notable features of the Wenchuan earthquake of May 12, 2008, and documents the geotechnical aspects of design and seismic damage to the 156-m-high Zipingpu CFRD during the earthquake. Based on the subsequent investigation following the earthquake, some key findings are presented here regarding the dynamic performance of the dam during the earthquake and resulting recommendations for seismic design in the future.

- 1) The Zipingpu CFRD dam is a zoned rockfill embankment dam, mostly resting on recent alluvium consisting of erratic boulders and gravel. The plinth and half of the upstream dam rest on the bedrock. Lenses of sand were stripped off from the foundation alluvium. High dry density of the rockfill was achieved by compaction using heavy vibratory rollers. In-situ monitoring indicated that the completed embankment was quite uniform.
- 2) The earthquake of May 12, 2008, produced about 40 s of strong shaking at the dam site. Two major effects of the earthquake were significant seismic non-uniform deformations and severe damage to joints in face slabs of the Zipingpu dam. In general, the damage to the dam, although serious in some parts, was minor overall and was easily repaired [4].
- 3) The seismic densification of rockfill resulted in the non-uniform residual deformation and discontinuous contact deformation, posing a major threat to the seepage control system as well as to the safety of the dam. This was largely attributed to the dynamic response of materials and structures under conditions such as cyclic loading, constrained boundaries, whiplash and traveling waves.
- 4) The predominant seismic motion along the dam axis intensified the interaction between the embankment and the abutments. The interaction as well as the non-uniform residual deformation is believed to have been responsible for extensive damage to face slabs, causing compression of concrete, dislocation and opening of joints. More flexible joints could be incorporated into face slabs to buffer the dynamic impacts and to adapt to large deformations. The poorly-performing lateral construction joints could be replaced by vertical construction joints.
- 5) The Zipingpu CFRD was structurally stable and safe even though it was subjected to seismic shaking at a greater magnitude than the design seismicity. The safety of the dam during the earthquake may be attributed to several major factors. (1) Careful zoning and compaction of rockfill, along with shallow-gradient downstream slopes, contributed to the safety of the dam. (2) The dam is 17 km away from the epicenter and rests on the very footwall of the reactivated causative faults; nevertheless, the dam site was also kept away from the two closest faults. This design consideration prevented the dam from experiencing extreme seismic effects. (3) The strongest ground motion was not in the transverse

- direction, and at the time of the earthquake the water level in the reservoir was close to the dead water level.
- 6) Controlling of deformation induced by earthquakes is crucial to the seismic safety of high embankment dams. However, it is also one of the most challenging tasks to cope with. So far in seismic design, the safety of a dam cannot be quantitatively evaluated in terms of the deformation of and damage to the embankment dam. Great effort is needed to better understand the dynamic response of the dam so as to establish a framework for interpreting intricate relationships between the seismic safety and earthquake-induced damage to high embankment dams.

Acknowledgments

This research work was funded by the National Basic Research Program of China (2013CB035902), the National Natural Science Foundation of China (51038007) and the State Key Laboratory of Hydroscience and Engineering Projects under Grant nos. 2013-KY-04 and 2014-KY-03.

References

- [1] Zhang J-M, Zhang BY. Geotechnical aspects of high embankment dams in China. Keynote lecture. In: Leung CF, et al., editors. Proceedings of the 12th Asian regional conference on soil mechanics and geotechnical engineering, vol. 2; 2004. p. 1197–214.
- [2] Yang ZY, Zhao QS, Fang GD. State-of-the-art of technology for hydrostructure in China. *Tech Earth-Rockfill Dam* 2012;17–24 [in Chinese].
- [3] Chen HQ. Earthquake resistance of large dams. In: Pan JZ, He J, editors. Large dams in China: a fifty-year review; 2000. p. 723–95.
- [4] Chen HQ. Lessons learned from Wenchuan earthquake for seismic safety of large dams. *Earthq Eng Eng Vib* 2009;8(2):241–9.
- [5] Guan ZC. Seismic protection basis and selection standard of high embankment dams. *Water Resour Plan Des* 2009;5:1–3 [in Chinese].
- [6] Chengdu Hydroelectric Investigation & Design Institute of SPC. A preliminary design report on risk control and reinforcement of the Zipingpu hydraulic project (geological part); 2009 [in Chinese].
- [7] China Earthquake Disaster Prevention Center. Institute of Earthquake Prediction. China Seismological Bureau. Check report on aseismic safety evaluation of the dam site of the Zipingpu hydraulic project, Minjiang River, Sichuan Province; 2009 [in Chinese].
- [8] Guan ZC. Investigation of the 5.12 Wenchuan earthquake damages to the Zipingpu Water Control Project and an assessment of its safety state. *Sci China Ser E: Technol Sci* 2009;52(4):820–34.
- [9] Ishihara K. Performances of rockfill dams during recent large earthquakes. In: Proceedings of the fifth international conference on recent advances in geotechnical earthquake engineering and soil dynamics (California); 2010. p. 1–11.
- [10] Li YH, Wang P, Cao R. Preliminary damage investigation of high embankment dams during the Wenchuan earthquake. In: Analysis and investigation on seismic damages of projects subjected to the Wenchuan Earthquake; 2009. p. 427–34 [in Chinese].
- [11] Song SW, Cai DW. Earthquake damage phenomena and deformation monitoring analysis for concrete faced rockfill dam at Zipingpu project during the Wenchuan earthquake. *Chin J Rock Mech Eng* 2009;28(4):841–9 [in Chinese].
- [12] Wang JL, Xu XT, Wang XL, Huang XF. Monitoring analysis of influence of Wenchuan 8.0 earthquake on talus slope stability at left bank in front dam of the Zipingpu hydraulic project. *Chin J Rock Mech Eng* 2009;28(6):1279–87 [in Chinese].
- [13] Water Resources and Hydro-power Planning & Design General Institute. A report on damage investigation and preliminary analysis of large and medium-sized hydropower projects (over 30 MW) within the Wenchuan earthquake disaster area; 2009 [in Chinese].
- [14] Wieland M. The effects of the May 12, 2008 Wenchuan Earthquake on large storage dams. *WASSERWIRTSCHAFT* 2009;99(9):10–5.
- [15] Yang ZY, Zhang J-M, Gao XZ. A primary analysis of seismic behavior and damage of the Zipingpu CFRD during the Wenchuan earthquake. *Water Power* 2009;35(7):30–3 [in Chinese].
- [16] Zhang GM, Ma HS, Wang H, Li L. Active tectonic blocks and strong earthquakes in the continent of China. *Sci China Ser D: Earth Sci* 2004;34(7):591–9 [in Chinese].
- [17] Zhao JM, Liu XS, Wen YF. Analysis of earthquake damage of the Zipingpu dam in the Wenchuan earthquake and the study proposal on the anti-earthquake and disaster reduction of high earth-rock dam. *Water Power* 2009;35(5):11–4 [in Chinese].
- [18] Zou DG, Zhou Y, Ling HI, Kong XJ, Xu B. Dislocation of face-slabs of zipingpu concrete face rockfill dam during Wenchuan earthquake. *J Earthq Tsunami* 2012;6(2):1–17.
- [19] Zhang J-M, Yang ZY, Gao XZ, Tong ZX. Lessons from Damages to High Embankment Dams in the May 12, 2008 Wenchuan Earthquake. In: Proceedings of the GeoShanghai International 2010, vol. 201. Keynote Lecture. ASCE Geotechnical Special Publications; 2010. p. 1–31.
- [20] Ge SM, Liu MA, Lu N, Godt JW, Luo G. Did the Zipingpu Reservoir trigger the 2008 Wenchuan earthquake? *Geophys Res Lett* 2009, 76–80;36.
- [21] Klose CD. Evidence for anthropogenic surface loading as trigger mechanism of the 2008 Wenchuan earthquake. *Environ Earth Sci* 2012;66(5):1439–47.
- [22] Wang HL, Zhang XD, Zhou LQ, Xu XF, Yang ZG, Lu X, et al. Study on the relationship between fluid infiltration and Q(s) tomography of the crust in Zipingpu Reservoir Area. *Chin J Geophys: Chin Ed* 2012;55(2):526–37 [in Chinese].
- [23] Gahalaut K, Gahalaut VK. Effect of the Zipingpu reservoir impoundment on the occurrence of the 2008 Wenchuan earthquake and local seismicity. *Geophys J Int* 2010;183(1):277–85.
- [24] Liu Y. Study on construction material for concrete faced rockfill dam at Zipingpu project. *Sichuan Water Power* 2003;22(2):63–71 [in Chinese].
- [25] Song YG, Deng LS, Cai DW, Liu DW, Wang K. Monitoring for concrete faced rockfill dam settlement during construction of Zipingpu project. *Sichuan Water Power* 2006;25(1):21–7 [in Chinese].
- [26] Wu CG. Embankment quality control of CFR dam in Zipingpu project. *Sichuan Water Power* 2006;25(1):12–4 [in Chinese].
- [27] Specifications for Seismic Design of Hydraulic Structures SL203-97. The People's Republic of China Electric Power Industry Standard. Beijing: China Water Power Press; 1997.
- [28] Luo G, Zhang J-M. 3-D seismic response analysis for Zipingpu concrete-faced rockfill dam. In: Proceedings of the fifth international conference on case histories in geotechnical engineering, USA; 2004. No. 2.11.
- [29] Kong XJ, Zhou Y, Zou DG, Xu B, Yu L. Numerical analysis of dislocations of the face slabs of the Zipingpu concrete faced Rockfill Dam during the Wenchuan earthquake. *Earthq Eng Eng Vib* 2011;10(4):581–9.
- [30] Liu ZP, Chi SC. Analysis on residual strain of Zipingpu Concrete Faced Rockfill Dam after Wenchuan earthquake. *Earthq Eng Eng Vib* 2013;12(2):221–8.
- [31] Newmark NM. Effects of earthquakes on dams and embankments. *Rankine Lect, Geotech* 1965;15(2):139–60.
- [32] Seed HB, Lee KL, Idriss IM, Makdisi FI. The slides in the San Fernando dams during the earthquake of February 9. *J Geotech Eng* 1971;101(GT7):651–88.
- [33] Serff N, Seed HB, Makdisi FI, Chang CK. Earthquake Induced Deformations of Earth Dams. Report No. EERC/76-4. Berkeley: Earthquake Engineering Research Center, University of California; 1976.
- [34] Kartal ME, Bayraktar A. Non-linear earthquake response of CFR DAM-reservoir–foundation systems. *Math Comput Model Dyn Sys* 2013;19(4):353–74.